

NJC

Accepted Manuscript



This is an *Accepted Manuscript*, which has been through the Royal Society of Chemistry peer review process and has been accepted for publication.

Accepted Manuscripts are published online shortly after acceptance, before technical editing, formatting and proof reading. Using this free service, authors can make their results available to the community, in citable form, before we publish the edited article. We will replace this *Accepted Manuscript* with the edited and formatted *Advance Article* as soon as it is available.

You can find more information about *Accepted Manuscripts* in the [Information for Authors](#).

Please note that technical editing may introduce minor changes to the text and/or graphics, which may alter content. The journal's standard [Terms & Conditions](#) and the [Ethical guidelines](#) still apply. In no event shall the Royal Society of Chemistry be held responsible for any errors or omissions in this *Accepted Manuscript* or any consequences arising from the use of any information it contains.



www.rsc.org/njc

ARTICLE

Nucleolipids as building blocks for the synthesis of ^{99m}Tc -labeled nanoparticles functionalized with folic acid

Cite this: DOI: 10.1039/x0xx00000x

Received 00th January 2012,
Accepted 00th January 2012

DOI: 10.1039/x0xx00000x

www.rsc.org/

Khalid Oumzil,^{a, b} Salim Khiati,^{a, b} Michel Camplo,^c Marc Koquely,^{a, b} Krishna Chuttani,^d Shubhra Chaturvedi,^d Anil K. Mishra,^{d,*} and Philippe Barthélémy^{a, b,*}

The development of drug delivery nanocarriers is emerging as a promising therapeutic tool to transport anti-cancer agents to tumors. In this contribution, preparation of nanoparticles (NPs), highly loaded with cisplatin using the bio-inspired hybrid nucleoside-lipids has been reported. The construction of these NPs using a “layer-by-layer” approach allows a surface functionalization with polyethylene glycol and targeting moieties. Uridine moieties were pegylated for folic acid (FA) functionalisation to render specificity for active targeting. The uridine moieties at the surface of the nanoparticle act as ligands for ^{99m}Tc radiolabeling, whereas the lipid chains maintain the structure of the nanoparticle. In vitro, these hybrid NPs are stable and actively internalize in two different cell lines overexpressing folic acid receptor. In vivo scintigraphy shows that nucleolipids functionalized NPs notably improved the pharmacokinetic profile of cisplatin (enhanced blood circulation time) and accumulated in tumor xenografted mice model.

1. Introduction

The treatment of numerous human diseases is limited by the inadequacy to deliver active pharmaceutical ingredient (API) in such a way that most API molecules will selectively reach the desired targets at optimal drug concentrations and with minimal collateral damage. Most APIs distribute throughout the whole body, which results in general toxicity and poor acceptance by patients. Hence, to improve treatment, it is necessary to increase both the blood stream stability and the selective targeting of APIs for diseased cells by creating novel formulations. Such advanced formulations would overcome the biological barriers that prevent APIs efficiently to reach their targets.

In the case of human cancer treatment, development of efficient APIs along with the improvement of drug selectivity for cancerous cells remains a challenge. Several strategies are currently under investigation, including development of new drug-delivery systems (DDS).¹

As an example of API in the treatment of malignancies, cisplatin is one of the most widely used and effective cytotoxic agent. This drug is also currently used in combination with other drugs, as first-line treatment against cancers of the lung, head and neck, ovaries, oesophagus, stomach, colon, bladder, testis, cervix, uterus and as second-line chemotherapy against other advanced cancers such as cancer of the pancreas, liver,

kidney, prostate as well as against glioblastomas, metastatic melanomas. However, the clinical use of this drug is limited due to the emergence of intrinsic and acquired resistance, and severe side effects, such as acute nephrotoxicity and chronic neurotoxicity. Its severe side effects arise from induction of apoptosis in various cell types in normal tissue in treated patients especially in peripheral nerves, renal tubules, bone marrow and gastrointestinal tract.

Thus, numerous DDS have been investigated, including polymeric micelles,²⁻⁵ liposomes,⁶ and nanoparticles⁷⁻¹⁰. Despite the huge efforts devoted to the development of novel DDS, the pharmacokinetic profiles, the stability of the API in physiological conditions and biodistribution have to be improved by novel advanced DDS approaches.

^{99m}Tc Technetium (^{99m}Tc) is the most attractive radioisotope because of its ideal nuclear properties, its easy availability worldwide through a radionuclide generator system along with feasibility for development of novel and versatile labeling techniques. ^{99m}Tc accounts for about 80% of the nuclear medicine tests in clinic worldwide;¹¹ thus it is commonly used for nanoparticle labeling^{12,13}. ^{99m}Tc and ^{111}In have long track records for use in drug development as SPECT imaging agents.¹⁴ Considering the above, the potential of ^{99m}Tc for labeling the developed nanoparticles (NP-PEG_{FA}) has been exploited.

Recently, we reported that hybrid nucleoside-lipids (NLs) allowed the efficient nano-encapsulation of cisplatin.¹⁵ In this new contribution, we demonstrate advanced formulations featuring new bio-inspired pegylated NLs with targeting moiety that can be labeled with ^{99m}Tc in the absence of DOTA (1,4,7,10-tetraazacyclododecane-1,4,7,10-tetraacetic acid). Such functionalized and labeled nanoplatfoms can address pharmacokinetic and biodistribution issues. NPs were assembled using a bottom up approach involving positive and negative nucleoside-lipids (NLs), pegylated nucleoside-lipids (NL-PEG₂₀₀₀ and NL-PEG₃₀₀₀-FA) and then subjected to ^{99m}Tc labeling for in vivo visualization of uptake and release pattern of API. The present study shows that ^{99m}Tc-labeled cisplatin nanoparticles functionalized with folic acid (^{99m}Tc-NP-PEG_{FA}) enhances the half-life of cisplatin in vivo and accumulate in tumor tissue.

2. Experimental

2.1. Synthetic procedures

Synthesis of compound 2. PEG₃₀₀₀ (400 mg, 1eq.), 2',3'-dioleoyluridine 1 (124 mg, 1.2eq.), N,N'-Dicyclohexylcarbodiimide (50 mg, 2eq.) and 4-(Dimethylamino)pyridine (15 mg, 1eq.) were dried for 1 h under high vacuum. The compounds were then dissolved under nitrogen in 5 mL of anhydrous methylene chloride (DCM). The mixture was stirred for overnight at room temperature under nitrogen. The dicyclohexylurea (DCU) was filtered and the solvent was removed. The product 2 was isolated after purification using LH20 size exclusion column in (DCM/MeOH 50:50). Yield: 84%. MALDI MS: Product 2, Cal Mw=4072, found Mw=4073.

Synthesis of compound 3. To a solution of DOU-PEG₃₀₀₀-NHBoc 2 (393 mg, 0.13mmol) in DCM (2 mL) was added TFA (5 mL) at 0 °C. The mixture was stirred for 4 h at room temperature. The solvent was evaporated and the product 3 was isolated after purification on LH20 size exclusion column in (DCM/MeOH 50:50). Yield: 94%. MALDI MS: Product 3, Cal Mw=3972, found Mw=3973.

Synthesis of compound 4 (DOU-PEG₃₀₀₀-FA). To a solution of DOU-PEG₃₀₀₀-NH₂ 3 (136 mg, 1eq.) in 2.5 mL of DMSO/pyridine (4/1) was added DCC (42 mg, 6 eq) and folic acid (45 mg, 3 eq). The mixture was stirred for overnight at room temperature under nitrogen. The DCU was filtered and the solvent was removed. The product 4 was isolated after purification using LH20 size exclusion column in (DCM/MeOH 50:50). Yield: 70%. MALDI MS: Product 4, Cal Mw=4395, found Mw=4391.

2.2. Preparation of cisplatin nanoparticles.

Cisplatin anionic nanoparticles. Cisplatin diluted in deionized (DI) water (5 mM) was incubated at room temperature for 48 hours under stirring. Dry lipid film composed of equimolar amounts of DOPC and diC₁₆-3'-dT²⁸ (1.2 mmole) was incubated overnight at room temperature with 1.2 mL of the 5mM aqueous solution of cisplatin. The mixture was subjected

to 10 cycles of freezing-thaw using ethanol/dry ice (-70°C) and warm water bath (55 °C). The resulting solution was sonicated prior to centrifugation at 10,000 rpm for 5 min in order to remove liposomes in supernatant. Anionic nanoparticles in pellet were suspended in 1 mL of DI water.

Cisplatin cationic nanoparticles. Anionic nanoparticles in 1 mL of DI water were added to a dry positively charged nucleolipid (DOTAU) film for 2 hours at 37°C under stirring. A 10,000 rpm centrifugation (5 min) was performed to remove the supernatant. Cationic nanoparticles in pellet were then diluted in 1 mL of DI water.

Concentration measurement. 50 µL of nanoparticles were dissolved in 5 mL of DI water with nitric acid (1%). After incubation overnight at room temperature, cisplatin concentration was evaluated with Inductively Coupled Plasma Atomic Emission Spectroscopy (ICP-AES) using a cisplatin range from 0.2 mg/L to 1 mg /L.

Transmission Electronic Microscopy (TEM). Nanoparticles were visualized by negative staining microscopy. 10 µL of nanoparticles (1 mM) were transferred to a carbon-coated copper grid for ten minutes. The sample was then dried and stained with 2.5 % (W/W) of uranyl acetate in water for five minutes. The specimens were observed with a Hitachi H 7650 electron microscope.

Particle size and zeta determination. Particle zeta and size were determined using a Zetasizer 3000 HAS MALVERN. Experiments were realized with 50 µL of the nanoparticles diluted in 1.2 mL of DI water and measurements were performed at 25°C.

2.3 Radiolabeling of nanoparticles

Preparation of ^{99m}Tc-Labeled Nanoparticle functionalized with folic acid (^{99m}Tc-NP-PEG_{FA}). The labeling with ^{99m}Tc was carried out as per the guidelines approved for use of low level radioactivity. [Na^{99m}TcO₄]⁻ was obtained from a commercial ⁹⁹Mo/^{99m}Tc generator (BRIT). 200 µl of ^{99m}Tc-pertechnetate (55 MBq) using 100 µL stannous chloride (1mg/mL in 10% acetic acid solution) was added to the suspension of nanoparticles functionalized with folic acid (300 µl, 1.6 mg) and mixed thoroughly. It was allowed to stand for 5 min at room temperature and then subjected to estimation of radiochemical purity by ascending instant thin layer chromatography (ITLC-SG) using silica gel impregnated fiber sheets as the stationary phase. The mobile phases used were 100% acetone, 0.9% saline and pyridine: acetic acid: water (3:5:1.5). Approx. 2-3 µl of the labeled preparation was spotted on separate ITLC-SG strips and developed in respective solvents. Each strip was cut into two halves and radioactivity in each segment was counted in Capintec, USA Gamma counter. In both the solvents (100% acetone, 0.9% saline) the labeled cisplatin nanoparticles functionalized with folic acid remained at the point of application (R_f= 0) whereas free pertechnetate R_f was 0.9-1.0. Pyridine: acetic acid: water (3:5:1.5) was used for correction due to radio-colloids.

Stability of the ^{99m}Tc labeled NPs ($^{99m}\text{Tc-NP-PEG}_{\text{FA}}$). The in vitro stability was done by spotting 2-3 μL of the labeled preparation on ITLC-SG strip, which was run in 100% acetone. The strip was cut into two halves and counts for both halves were taken separately in gamma counter. Labeling efficiency of the NP ($R_f=0$) was calculated as the ratio of counts in the lower part of ITLC and the total counts obtained in the two halves. The upper ITLC counts correspond to the free pertechnetate, as mentioned above. The results have been expressed in terms of percentage. For in vivo stability, 2-3 μL of blood sample withdrawn in blood kinetics study (mentioned below) was spotted, run in acetone and labeling efficiency was determined as above.

2.4. In vitro studies

Cisplatin release in Fetal Bovine Serum (FBS) study.

20 μL of the nanoparticles solution and 130 μL of FBS were mixed and incubated at 37°C under a 300 rpm stirring. For each time (0, 1, 2, 3, 18 and 24 h), the corresponding tube was centrifugated (14,000 rpm) for 10 min and cisplatin released was measured in 50 μL of the supernatant.

Flow Cytometry Analysis of IGROV1 and SKOV3 for folic acid receptor expression. The cells (IGROV1 and SKOV3) are cultured in Dulbecco's Modified Eagle's Medium (DMEM, Invitrogen) and supplemented with 10% fetal bovine serum (FBS, invitrogen) at 37°C in a 5% CO_2 atmosphere. Cells were split every 4–5 days to maintain monolayer coverage. Cells on monolayer in T75 Falcon were trypsinized and washed two times with cold PBS. 1×10^6 cells were transferred into each three Eppendorf tubes and centrifuged. The pelleted cells were resuspended in 200 μL of PBS with 0.1% BSA. The first tube, as control, incubated without antibodies. The second tube was incubated with fluorescent secondary antibody (Goat anti mouse alexafluor 488) without the primary antibody. The third tube was incubated with primary antibody (mouse anti-FR α) for 30 min and secondary antibody for 15 min. Cells were resuspended in 400 μL of PBS and analysed by FACS.

Cytotoxicity Analysis. Cytotoxicity was assessed with formazan-based proliferation assay (Cell Titer 96 Aqueous One Solution Cell Proliferation Assay kit, Promega). Human ovarian carcinoma cell line IGROV1 and SKOV3 were used for this study. Cells were seeded in each well of a 96-well plate (2500 cells/well) and allowed to attach overnight. The cells were incubated with concentration ranges of 500, 250, 100, 10, 1, 0.1, 0.01, and 0.0001 μM of nanoparticles for the defined time. After treatment, cells were washed twice with PBS and incubated in 100 μL of medium with serum. Three days after, 20 μL of the MTS substrate was added to each well, and the plates were incubated for 2–4 h at 37°C in 5% CO_2 incubator. Cell death was performed using a multiwell plate reader at 490 nm.

2.5 In vivo study with $^{99m}\text{Tc-NP-PEG}_{\text{FA}}$.

Normal, healthy, New Zealand albino rabbits weighing 2.0-2.5 kg and Balb/c mice (aged 2 months, weighing 25 - 28 grams)

were used. All animals were housed in the animal facility with room temperature $22-25^\circ\text{C}$, 12-h day-night cycle and had free access to food and water. The experiments on animals were carried as per the guidelines compiled by the Committee for the Purpose of Control and Supervision of Experiments on Animals, Ministry of Culture, Government of India and all the protocols were approved by the institutional animal ethics committee of the Institute of Nuclear Medicine and Allied Science (approval reference: INM/DASQA/IAEC/09/015).

Pharmacokinetic studies for $^{99m}\text{Tc-NP-PEG}_{\text{FA}}$.

The blood kinetic was carried out in New Zealand rabbits. In each rabbit, 18.5 MBq of labeled compound (free cisplatin and cisplatin nanoparticles) was injected through the dorsal ear vein and blood samples from the other ear vein were withdrawn at different time intervals starting from 15 min up-to 24 h.

Biodistribution Studies.

Each Balb/c mice was injected 3.7 MBq activity of radiolabeled nanoparticles through the tail vein. After the time points 1, 2, 4, 6 and 24 h post injection, the animals ($n=5$ in each group) were humanely sacrificed and blood was collected by the cardiac puncture. The organs/ tissues of interest were collected and washed with normal saline and dried. Organs and tissues were weighed and their corresponding radioactivity was measured using gamma counter (Caprac R Capintech) along with the injection standard. The percentage of injected dose per gram of tissue (%ID/g) was calculated.

Scintigraphic Studies.

In-vivo SPECT whole body images, were acquired using dual head SPECT-CT SYMBIA T2, SIEMENS gamma camera. 18.5 MBq activity of $^{99m}\text{Tc-NP-PEG}_{\text{FA}}$ was injected in Ehrlich ascites tumor (EAT) bearing mice through tail vein. Static acquisitions were acquired in anterior mode. Semi quantitative analysis was generated from region of interest through Entegra® software.

3. Results

3.1. Construction of the nanoparticles (NPs).

Design of ^{99m}Tc -Labeled NPs functionalized with PEG and FA targeting moieties. Folic acid has been widely used as a ligand for targeted therapeutic approaches against cancers, including the delivery of chemotherapeutic agents, toxins, DNA, siRNA, liposomes, micelles, dendrimers and nanoparticles.¹⁶ For this reason, FA has been covalently attached to a pegylated-nucleolipid, which has been inserted at the NP surface for the purpose of selectively targeting to tumors. In this contribution, we propose a simple procedure to prepare ^{99m}Tc -labeled NPs functionalized with PEG and FA targeting moieties in order to improve the pharmacokinetic profile of cisplatin and its biodistribution. Cisplatin nanoparticles were labeled with ^{99m}Tc by direct labeling method. As reported in the literature labeling of nanoparticles with ^{99m}Tc can be conveniently performed by stannous-based reduction.^{17,10}

^{99m}Tc labeled NPs functionalized with PEG and folate ($^{99m}\text{Tc-NP-PEG}_{\text{FA}}$) were prepared using a 3 steps procedure: i) encapsulation of the cisplatin in the solid state using a

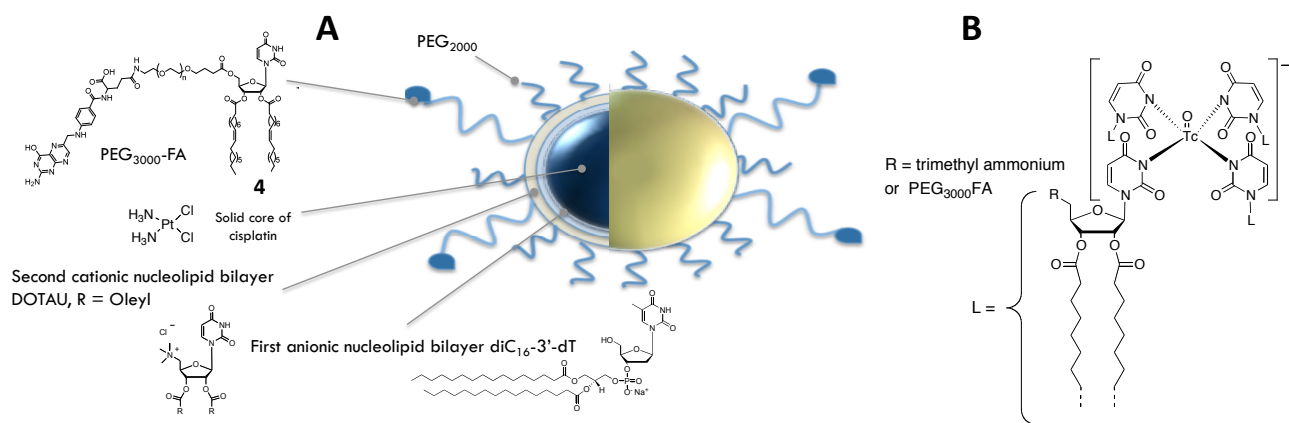


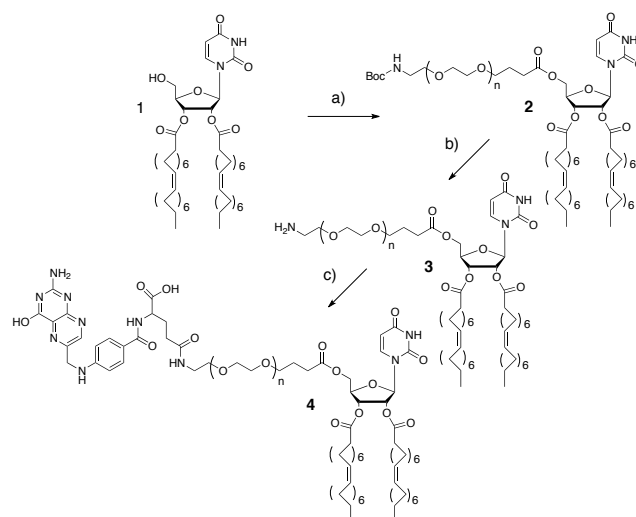
Figure 1. (A) Schematic drawing of cisplatin loaded nanoparticles featuring PEG2000 and PEG3000-FA, chemical structures of an anionic nucleotide-lipid, the thymidine 3'-(1,2-dipalmitoyl-*sn*-glycero-3-phosphate) (diC16-3'-dT), a cationic-nucleoside-lipid DOTAU (2',3'-dioleoyl-5'-deoxy-5'-trimethyl-ammonium-uridine) and folate PEG nucleolipid used in this study. (B) Proposed ^{99m}Tc -Pyrimidine complex allowing the labelling of the NPs used in this study (^{99m}Tc -NP-PEGFA).

combination of anionic nucleotide-lipid²⁸: diC16-3'-dT (thymidine 3'-(1,2-dipalmitoyl-*sn*-glycero-3-phosphate)) and a cationic nucleoside-lipid DOTAU¹⁸ (2',3'-dioleoyl-5'-deoxy-5'-trimethyl-ammonium-uridine), which provide stable positively charge NPs (NP+)¹⁵; ii) insertion of PEG derivatives and folic acid targeting moiety (Figure 1A) and iii) labeling of NPs using ^{99m}Tc .

Synthesis of DOU-PEG₃₀₀₀-FA. In order to insert FA targeting moieties at the surface of the NPs a new pegylated nucleolipids (DOU-PEG₃₀₀₀-FA, compound **4** Figure 1A) was synthesized using a 3 steps procedure starting from nucleoside lipid **1**.¹⁹ Briefly state, the primary hydroxyl at the 5' group of starting material **1** was reacted with BOC-NH-PEG carboxylate reagent to provide intermediate **2** in 84% yield. Deprotection of BOC lead to primary amine (compound **3**), which was coupled with folic acid to give the expected product **4** (DOU-PEG₃₀₀₀-FA) in 70% yield (Scheme 1).

Preparation and characterization of ^{99m}Tc labeled NPs functionalized with PEG and folate targeting moieties. The positive NP+ nanoparticles prepared using a similar procedure as previously published¹⁵ were incubated for 2 h at 37 °C in the presence of a mixture of DOU-PEG₂₀₀₀ and DOU-PEG₃₀₀₀-AF (2.25%, 0.25%, mol/mol relative to DOTAU). This step provided pegylated nano-objects with a zeta-potential of + 24.3 mV (Figure SI1), which is lower than starting naked NP+ (48.4 +/- 7.6 mV).¹⁵ Dynamic light scattering (DLS) experiments indicate the formation of nano-objects of 100 nm, (PDI=0.235, Figure SI2), which is in accordance with oblong nanoparticles observed on the transmission electronic microscopy (TEM) images (Figure SI3).

To determine the NPs stabilities, the kinetics of cisplatin released was measured at 37°C in the presence of serum (Figure 2). As previously reported NP+ featuring a multilayer system composed of diC16-3'-dT and DOTAU exhibited an increased stability compared to negative NP⁻. With less than 65 % of



Scheme 1. Synthetic route to DOU-PEG₃₀₀₀-FA (compound **4**), a) PEG₃₀₀₀-NHBoc, DCC, DMAP, DCM, overnight, 25 °C, 84% yield. b) TFA, DCM, 4 h, 25 °C, 94% yield. c) Folic acid, DCC, DMSO/Pyr, overnight, 25 °C, 70% yield.

release for NP-PEG and after 24 hours of incubation in the presence of serum at 37°C, NP-PEG are the most stable of the NP series (100% and 90% of release for NP- and NP+, respectively). This result indicates that the insertion of PEG at the NP surface does not destabilize the NP supramolecular systems and improve their stability in the presence of serum.

Radiolabeling evaluation. Next, the direct labeling of these cisplatin loaded nanoparticles was carried out with ^{99m}Tc using stannous chloride as reductant for pertechnetate to lower the oxidation state (from +7 to +5) of ^{99m}Tc which forms complex with uridine moieties. The labeling efficiency, expressed in terms of percentage, was found to be more than 97% as confirmed by paper chromatography using ITLC-SG (silica gel

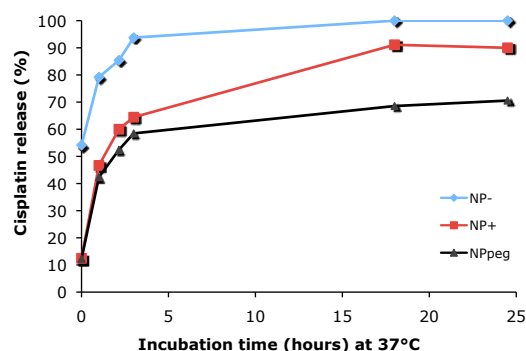


Figure 2. Cisplatin release from nanoparticles after incubation at 37°C in serum under 300 rpm agitation. In blue, anionic nanoparticles formulated with diC16-3'-dT/DOPC (NP-), in red, cationic nanoparticles stabilized with both diC16-3'-dT/DOPC and DOTAU (NP+) and in black NP+ nanoparticles functionalized with PEG (NP-PEG).

impregnated instant thin layer chromatography) as the stationary phase and 100% acetone (Figure 3A), 0.9% saline and pyridine: acetic acid: water (3:5:1.5) as the mobile phases. The labeled nanoparticles R_f was found to be 0 whereas free moiety (^{99m}Tc) migrated with the solvent front ($R_f=0.9-1.0$) in both solvents (100% acetone and 0.9% saline). For further correction, radioactivity due to radio-colloids was subtracted which was determined by running ITLC in pyridine: acetic acid: water (3:5:1.5) wherein, only the radio colloids remained at the bottom of the strip. By subtracting the counts of free moiety from the total counts (sum of colloid subtracted base counts and top counts) the percentage of effective labeling efficiency was calculated. The counts were acquired in a well type gamma counter (Capintec, USA) calibrated for ^{99m}Tc energy.

The high yield of labeling can be explained by the formation of ^{99m}Tc -Pyrimidine (Uridine) complexes (Figure 1B). Indeed, recently the formation of ^{99m}Tc -dihydroPyrimidinone was reported using stannous chloride in similar condition.²⁰ A proposed structure of ^{99m}Tc -Pyrimidine involving our uridine based NLs is presented in Figure 1C. ^{99m}Tc -Uridine anionic complex contains the $^{99m}\text{Tc}=\text{O}$ (+5 oxidation state) core. The coordination bonds between ^{99m}Tc and N atoms of four Uridine ligands (Nucleolipids located at the NP surface) are formed by the electron pairs from the nitrogen atoms. The ^{99m}Tc -Uridine complex proposed has a square pyramidal geometry with an apical $\text{Tc}=\text{O}$ bond and four nucleolipid ligands.

Stability of the ^{99m}Tc complexes.

The labeled complexes were highly stable both in *in-vitro* and *in-vivo* conditions as shown in Figure 3B. The high stability observed in the NPs despite the lack of DOTA moiety can be attributed to the numerous sites of complexation at the surface of the nanoparticles. In our system, uridine moieties of NLs are acting as ligands for ^{99m}Tc , whereas the lipid chains inserted in the nucleolipid layer maintain the ^{99m}Tc -Uridine complexes attached to the NPs.

3.2. In vitro evaluation of NPs.

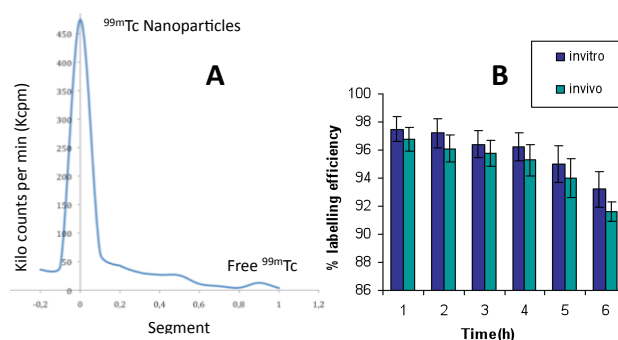


Figure 3. A) Counts plotted against different segments of ITLC strip developed in 100% acetone showing $R_f=0$ for ^{99m}Tc -labeled nanoparticles and $R_f=0.9-1.0$ for free ^{99m}Tc . B) *In vitro* and *in vivo* ^{99m}Tc labeling stability (% labeling efficiency) of ^{99m}Tc -NP-PEG_{FA} versus time.

Folic acid mediated internalization of NPs in cancer cells and cytotoxicity.

FA, which is uptaken by cells *via* folate receptors (FR), has been frequently used as a targeting ligand for the delivery of drugs and/or drug vehicles to cancer tissues due to the over expression of FR on many different human tumor cells, including ovarian, breast, cervical, lung, kidney, brain and colorectal and cancer cells.^{21,22}

To confirm the ability of the NP-PEG_{FA} to be internalized *via* folate-mediated receptors, two ovarian cancer cell lines (IGROV1 and SKOV3) have been selected for this study. Prior to the evaluation of the anti-cancer activities of the NP-PEG_{FA}, the level of FR expression was determined using FACS analyzes. The data collected show clearly an over expression of FR indicating the presence of FR at the surface both cell lines (Figure S17). Next, in order to evaluate the anticancer potential of the NP-PEG_{FA} we have determined the concentrations of novel cisplatin nanoparticles to obtain a 50% inhibition of proliferation (IC_{50} values in μM) against sensitive (IGROV1) and cisplatin resistant (SKOV3) ovarian cancer cell lines. Figure 4 shows the cytotoxic effects (IC_{50}) of free cisplatin and different NPs (non-pegylated cationic nanoparticles NP+, pegylated nanoparticles NP-PEG and pegylated nanoparticles featuring FA ligands NP-PEG_{FA}) against IGROV1 and SKOV3. As a general comment, in all cases the NPs exhibits increased cytotoxic activities with IC_{50} values lower than 1 μM and 8 μM in the case of NPs compared to 3.6 μM and 35 μM for free cisplatin, in IGROV1 and SKOV3, respectively. Interestingly, we also confirmed that the presence of FA ligands at the NP surface change the cytotoxicity efficacy of the nanoparticles in ovarian cell line. The analysis of the IC_{50} values indicate that folate enhance nanoparticles efficiency ($\text{IC}_{50}=0.368$ μM and 2.11 μM) compare to NP-PEG without folic acid ($\text{IC}_{50}=0.977$ μM and 7.33 μM) in both IGROV1 and SKOV3 cell line respectively.

These second generations of our NPs are more stable *in vitro* than the first generation reported previously. Also, NP-PEG_{FA} is active against cell over expressing FR. For further

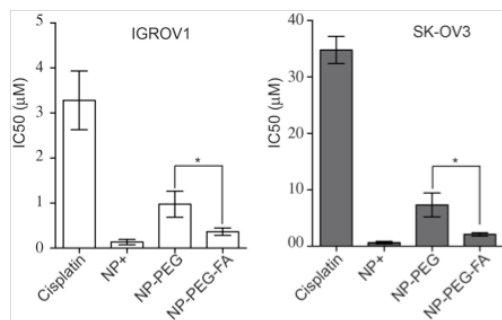


Figure 4. Summary of IC₅₀ of three independent experiments of sensitive (IGROV1) and cisplatin resistance (SKOV3) cell lines. Cells were treated at different concentration ranging from 500 μM to 0.1 nM for two hours and viability was measured by MTS assay three days later (t test, * $P < 0.05$).

characterization, we decide to evaluate this new generation of labeled NPs (NP-PEG_{FA}) *in vivo*.

In vivo evaluation of NPs.

Pharmacokinetic and Biodistribution of ^{99m}Tc labeled NPs (NP-PEG_{FA}).

The pattern for labeled nanoparticles obtained in the blood clearance study carried out in rabbits was observed to be biphasic (Figure S18). The pattern was initially fast, but after fifteen minutes the clearance becomes slow with 6.5 % of injected activity was seen in blood at 4h.

These results were compared with the blood kinetics study of free cisplatin in the same conditions with noticeable difference in the pharmacokinetic profile. Indeed, NP-PEG_{FA} significantly improved cisplatin pharmacokinetics *in vivo*. The blood kinetics of free cisplatin labeled with ^{99m}Tc also exhibited biphasic pattern but the clearance was appreciably faster with $t_{1/2}(\text{fast}) = 56$ min and $t_{1/2}(\text{slow}) = 10$ h 48 min as compared to its NP-PEG_{FA} which showed $t_{1/2}(\text{fast}) = 2$ h 10 min and $t_{1/2}(\text{slow}) = 18$ h 20 min (Figure S18).

The biodistribution was carried at different time points 1, 2, 4, 6 and 24 h (Figure 5). With respect to other organs, high uptake was seen in liver, spleen and kidney which were associated with excretion. Nanoparticles by virtue of their size are known to accumulate in liver and spleen. The effective build-up in the uptake was as early as 1 hour with % ID uptake of 1.03 (~85%) of maximum uptake.

Interestingly, a maximum uptake at the tumor site was obtained at 4 h with a dose value of 1.21 ± 0.11 % (%ID/g). At the same time point, muscle showed a value of 0.3 ± 0.04 (%ID/g), indicating that the uptake in tumor was 4 fold compared to muscle (Figure 6A).

Scintigraphic Studies of ^{99m}Tc labeled NPs (NP-PEG_{FA}). As revealed by the scintigraphic studies, the complex accumulated in liver depicting hepatobiliary route as the major excretory route. However, the tumor to muscle ratio was 4:1 (counts in the tumor region were 4 times more than the contralateral muscle) indicating that cisplatin ^{99m}Tc labeled NPs accumulate

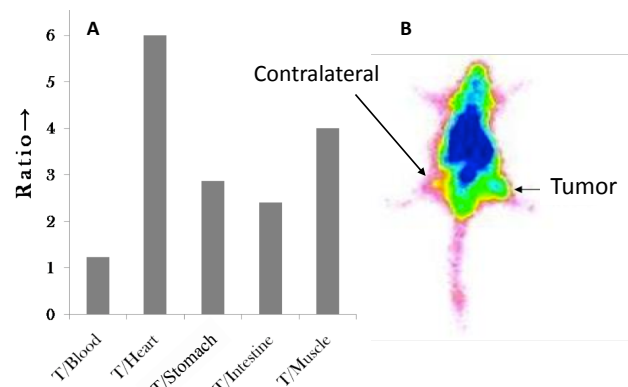


Figure 6. A) Dose ratios (% ID/g) in Tumor/Organ obtained from data presented in figure 5 (biodistribution). B) Scintigraphic image of ^{99m}Tc-NP-PEGFA in EAT mice at 4h post injection.

preferentially in the tumor compared to contralateral muscle (Figure 6B).

4. Discussion

We sought to develop theranostic nanoparticles that could improve the therapeutic index of cisplatin by enhancing the drug efficiency and decreasing its toxicity. The combination of nucleotides or nucleosides with lipids offers new formulating agents possessing unique supramolecular capabilities.²³⁻²⁷

These self-assembly properties render NPs ideal candidates for encapsulating platinum drugs. In a previous study we demonstrated that NPs could provide stable NPs featuring high drug loading capabilities and improved antitumoral activities, which are key issues in the field of drug delivery.¹⁶

^{99m}Tc is a well-known radioactive tracer used in many hospitals worldwide for imaging different tissues and tumors in humans. Hence, ^{99m}Tc labelling is a very attractive way to engineer nanomaterials, which could be useful in theranostic applications. In order to label cisplatin loaded nanoparticles and ensure their stability under physiological conditions, we first prepared and characterized ^{99m}Tc labeled NPs functionalized with new PEG nucleolipids featuring folate targeting moieties. We demonstrated that the insertion of PEG nucleolipid derivatives at the NP surface did not destabilize the NPs. Interestingly, despite the lack of ^{99m}Tc ligand such as DOTA, these nucleolipid based NPs feature numerous sites of complexation. Uridine moieties located at the surface of the nanoparticles are acting as ligands for ^{99m}Tc, whereas the lipid chains maintain the ^{99m}Tc-Uridine complexes attached to the NPs. Importantly, the blood kinetic of cisplatin was improved in the case of NPs compared with free cisplatin (biphasic kinetics: $t_{1/2}(\text{fast}) = 56$ min and $t_{1/2}(\text{slow}) = 10$ h 48 min, $t_{1/2}(\text{fast}) = 2$ h 10 min and $t_{1/2}(\text{slow}) = 18$ h 20 min for cisplatin and cisplatin loaded NPs, respectively). Targeted nanoparticles through the folate ligand bind to the FR receptor in the tumor, and as a result, is effectively “halted” in place through receptor binding. In non-targeted system, however, accumulation in tumor is due to repeated recirculation before becoming trapped

and accumulating in the tumor. An early uptake of activity (within 1 h) and high retention at the tumor site up-to 6 h can only be ascribed to receptor mediated endocytosis and clearly indicate folate mediated active targeting. In addition, the presence of folate ligands at the NP surface (NP-PEG_{FA}) also mediate the internalization of NPs in cells as demonstrated on two ovarian cancer cell lines (IGROV1 and SKOV3). Lastly but importantly, a favorable uptake of NPs was observed in tumor in comparison to heart, muscle, stomach and intestine (Figure 6).

5. Conclusions

In summary, we have provided a facile method for the preparation of ^{99m}Tc-labeled cisplatin nanoparticles functionalized with folic acid (^{99m}Tc-NP-PEG_{FA}). We have described the synthesis of a new PEG Nucleolipid featuring a folic acid as a targeting moiety (DOU-PEG₃₀₀₀-FA). The use of nucleolipids, including DOTAU, diC₁₆-3'-dT and DOU-PEG₃₀₀₀-FA allows formation of stable NPs, which can be efficiently and directly labeled using stannous chloride and pertechnetate reagents. The in-vitro and in-vivo studies demonstrate high stability of NPs and biphasic kinetic pattern for a sustained release of cisplatin. In similar conditions, the blood clearance of free cisplatin was faster as compared to the pegylated nanoparticles loaded with cisplatin, demonstrating the advantage of NP formulations in terms of pharmacokinetics. ^{99m}Tc-NP-PEG_{FA} also show accumulation at tumor site compared to muscles for development of efficient, non-toxic drug delivery systems. In vivo stability and scintigraphic study in Ehrlich Tumor bearing mice strongly highlight its strong intactness with the radioisotope as no stomach activity was seen in the image. Overall, the nanoparticles functionalized with folic acid developed in the course of the present study, demonstrate the feasibility of using nucleolipid formulations for in vivo delivery of anti cancer drugs. These formulations also provide a foundation for the development of novel radiotracer labeled NPs with potential theranostic applications.

Acknowledgements

This research was supported in part by the French National Agency (ANR) in the frame of its programmes EmergenceBio (project NANOVA, n°ANR-08-EBIO-013-01), and the Army Research Office. The authors thank the Bordeaux Imaging Center (BIC) and the Laboratoire d'Hydrologie-Environnement, University of Bordeaux for technical assistance during TEM observations and ICP-AES measurements, respectively.

Notes and references

^a INSERM U869, Bordeaux, F-33076, France.

^b Université de Bordeaux, Bordeaux, F-33076, France.

^c CINaM, Université de la méditerranée, 13288 Marseille cedex 9, France.

^d Division of Cyclotron and Radiopharmaceutical Sciences, Institute of Nuclear Medicine and Allied Sciences (INMAS), DRDO, Delhi, India.

† Electronic Supplementary Information (ESI) available: [DLS, zeta potentials, MS spectra, NMR, Blood Kinetic and TEM]. See DOI: 10.1039/b000000x/

- Cheng, Z., Al Zaki, A., Hui, JZ., Muzykantov, VR., and Tsourkas A. *Science* 2012; **338**, 903-910.
- Uchino, H., Matsumura, Y., Negishj, T., Koizumi, F., Hayashi, T., Honda, T., Nishivama, N., Kataoka, K., Naito, S., and Kakizoe, T. *British Journal of Cancer* 2005; **93**, 678-687.
- Santosh, A., Che-Ming, J. H., and Liangfang, Z. *Polymer-Cisplatin ACS Nano* 2010; **4**, 251-258.
- Tian, Y., Bromberg, L., Lin, S. N., Alan Hatton, T., and Tam, K. C. *J. Control. Release* 2007; **121**, 137-145.
- Kaida, S., Cabral, H., Kumagai, M., Kishimura, A., Terada, Y., Sekino, M., Aoki, I., Nishiyama, N., Tani, T., and Kataoka, K. *Cancer Res.* 2010; **70**, 7031-7041.
- Boulikas, T., and Vougiouka, M. *Oncology reports* 2004; **11**, 559-595.
- Dhar, S., Gu, F. X., Langer, R., Farokhzad, O. C., and Lippard, S. J. *Proc. Natl. Acad. Sci. U.S.A.* 2008; **105**, 17356-17361.
- Dhar, S., Kolishetti, N., Lippard, S. J., and Farokhzad, O. C. *Proc. Natl. Acad. Sci. U.S.A.* 2011; **108**, 1850-1855
- Paraskar, A. S., Soni, S., Chin, K. T., Chaudhuri, P., Muto, K. W., Berkowitz, J., Handlogten, M. W., Alves, N. J., Bilgicer, B., Dinulescu, D. M., Mashelkar, R. A., and Sengupta, S. *Proc. Natl. Acad. Sci. U.S.A.* 2010; **107**, 12435-12440.
- Reddy, L.H., Sharma, R.K., Chuttani, K., Mishra A. K., and Murthy R.R. *AAPS Journal* 2004; **6**, e23.
- Banerjee, S., Pillai, M.R., and Ramamoorthy, N. *Semin. Nucl. Med.* 2001; **31**, 260-277.
- Sandiford, L., Phinikaridou, A., Protti, A., Meszaros, L.K., Cui, X., Yan, Y., Frodsham, G., Williamson, P.A., Gaddum, N., Botnar, R.M., Blower, P.J., Green, M.A., and de Rosales. R.T.M. *ACS Nano* 2013; **7**, 500-512.
- de Rosales, R. T. M., Tavare, R., Glaria, A., Varma, G., Protti, A., and Blower, P. J. *Bioconjug. Chem.* 2011 ; **22**, 455-465.
- Phillips, W.T., Rudolph A.S., Goins, B., Timmons, J.H., Klipper, R., and Blumhardt, R. *Int. J. Rad. Appl. Instrum. B*, 1992; **19**, 539-547
- Khiati, S., Luvino, D., Oumzil, K., Chauffert, B., Camplo, M., and Barthélémy P. *ACS Nano* 2011; **5**, 8649-8655.
- Xia, W., and Low, P.S. *J. Med. Chem.* 2010; **53**, 6811-6824.
- Hass, F. J., Lee, P. S., and Lourenco, R.V. *J. Nucl. Med.* 1976; **17**,122.
- Chabaud, P., Camplo, M., Payet, M. D., Serin, G., Moreau, L., Barthélémy, P., and Grinstaff, M. *Bioconjugate Chem.* 2006; **17**, 466-472.
- Oumzil, K., Khiati, S., Grinstaff, M. W., and Barthélémy, P. *J. Control. Release.* 2011; **151**, 123-30.
- De, K., Chandra, S., Sarkar, B., Ganguly, S., and Misra, M. *J. Radioanal. Nucl. Chem.* 2010; **283**, 621-628.
- Leamon C.P. *Curr. Opin. Investig. Drugs* 2008; **12**, 1277-1286.
- Low, P. S. and Antony, A. C. *Adv Drug Deliv Rev.* 2004; **56**, 1055-1231.

- 23 Allain, V., Bourgaux, C., and Couvreur, P. *Nucleic Acids Res.* 2012; **40**, 1891-1903.
- 24 Gissot, A., Camplo, M., Grinstaff, M. W., and Barthélémy, P. *Org. Biomol. Chem.* 2008; **6**, 1324–1333.
- 25 Barthélémy, P. *C.R. Chimie* 2009; **12**, 171-179.
- 26 Rosemeyer, H. *Chem. Biodiversity* 2005; **2**, 977-1062.
- 27 Latxague, L., Dalila, M.J., Patwa, A. Sophia, Z., Chassande, O., Godeau, G., and Barthélémy P. *C.R. Chimie* 2012; **15**, 29–36
- 28 Khiati, S., Pierre, N., Andriamanarivo, S., Grinstaff, M. W., Arazam, N., Nallet, F., Navailles, L., and Barthélémy, P. *Bioconjugate Chem.* 2009; **20**, 1765-1772.